

Experimental-Computational Approach to Investigate Elastic Properties of Struvite

Dominik Sidorczyk¹, Łukasz Kołodziejczyk², Katarzyna Pernal¹, and Jolanta Prywer¹

¹Institute of Physics, Lodz University of Technology, ul. Wólczńska 219, 90-924 Łódź, Poland

²Institute of Materials Science and Engineering, Lodz University of Technology, Stefanowskiego 1/15, 90-924 Łódź, Poland

email: dominik.sidorczyk@dokt.p.lodz.pl



Crystals
2020

1. Introduction

Much research effort is devoted to struvite for various reasons. The main reason is that struvite is a major component of infectious urinary stones. Medicine deals with infectious urinary stones using, inter alia, extracorporeal shock wave lithotripsy (ESWL). Mechanical and elastic properties are important parameters for determining the optimal mechanical response of urinary stones to a shock wave. These properties indicate how urinary stones interact with the mechanical stresses produced by ESWL. In particular, moduli of elasticity are important parameters for determining the mechanical response of urinary struvite stones and hence the fragility of the stones under the influence of an extracorporeal shock wave. In addition, the elastic properties of struvite are essential to establish an optimal struvite removal strategy in wastewater treatment plant pipes using shock wave technology. This is an important point as struvite crystals easily precipitate at certain locations in the pipes of the wastewater treatment plant and then grow rapidly, leading to clogging of these pipes.

2. Main goals

The purpose of this research is to provide a combined theoretical and experimental investigations of properties of struvite, such as: elastic constants, in particular Kirchhoff modulus G , Young's modulus E and bulk modulus B . Theoretical calculations of the above properties of struvite were carried out by density functional methods using the CRYSTAL17 code [1], which is an ab initio quantum chemistry program. We also present the experimental values of Young's modulus obtained for a single struvite crystal and for a properly prepared tablet. Single crystal measurements are important in determining the property of struvite as a crystalline material. On the other hand, the tablet may be better at imitating urinary stone, as it is known that the stone is composed of a large number of small crystals that have aggregated together. In the presented work, we also compare the experimentally obtained values of Young's modulus with the calculated ones and, on this basis, we draw conclusions regarding reliability of the density functional methods applied to the dielectric material.

3. Growth process

Struvite (magnesium ammonium phosphate hexahydrate $MgNH_4PO_4 \cdot 6H_2O$) crystals were synthesized in sodium metasilicate gel by single diffusion gel growth technique. To prepare gel we used sodium metasilicate (Na_2SiO_3 — SMS), ammonium dihydrogenphosphate ($NH_4H_2PO_4$ — ADP) and magnesium acetate solution (CH_3COO)₂Mg. The chemicals were dissolved in distilled water. An aqueous solution of ADP of concentration of 0.5 M and SMS solution of specific gravity 1.07 were mixed together in appropriate amounts to adjust the pH of the mixture equal to 7.0. So prepared mixture was poured into tubes of 19 cm in length and 3 cm in diameter and left for gelation for 24 hours. After the gelation, 25 ml of magnesium acetate solution of 1 M was gently poured on the surface of newly-formed gel in respective tubes. The crystal growth usually lasted from three to four weeks. After this time the crystals of struvite of about 1 cm in size along the b -axis were observed.

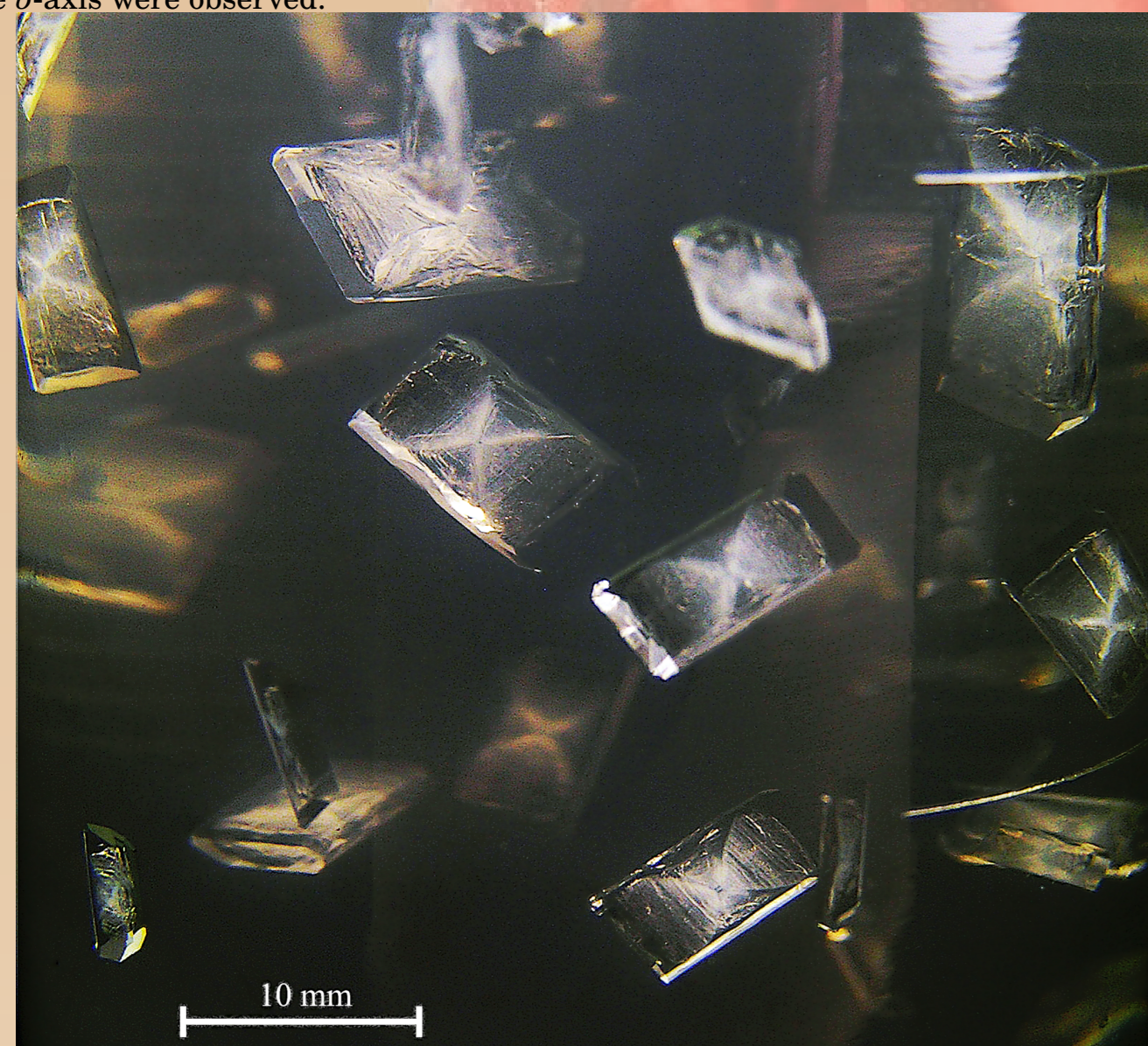


Figure 1. Struvite crystals in gel medium grown in our laboratory.

4. Crystal structure

Crystals grown in our laboratory were examined and identified as pure struvite by X-ray diffraction (XRD). Struvite belongs to the noncentrosymmetric point group $mm2$ of the orthorhombic system with space group $Pmn2_1$. The experimental lattice parameters are as follows: $a = 6.9650$ Å, $b = 6.1165$ Å, $c = 11.2056$ Å and volume $V = 477.38$ Å³ [2].

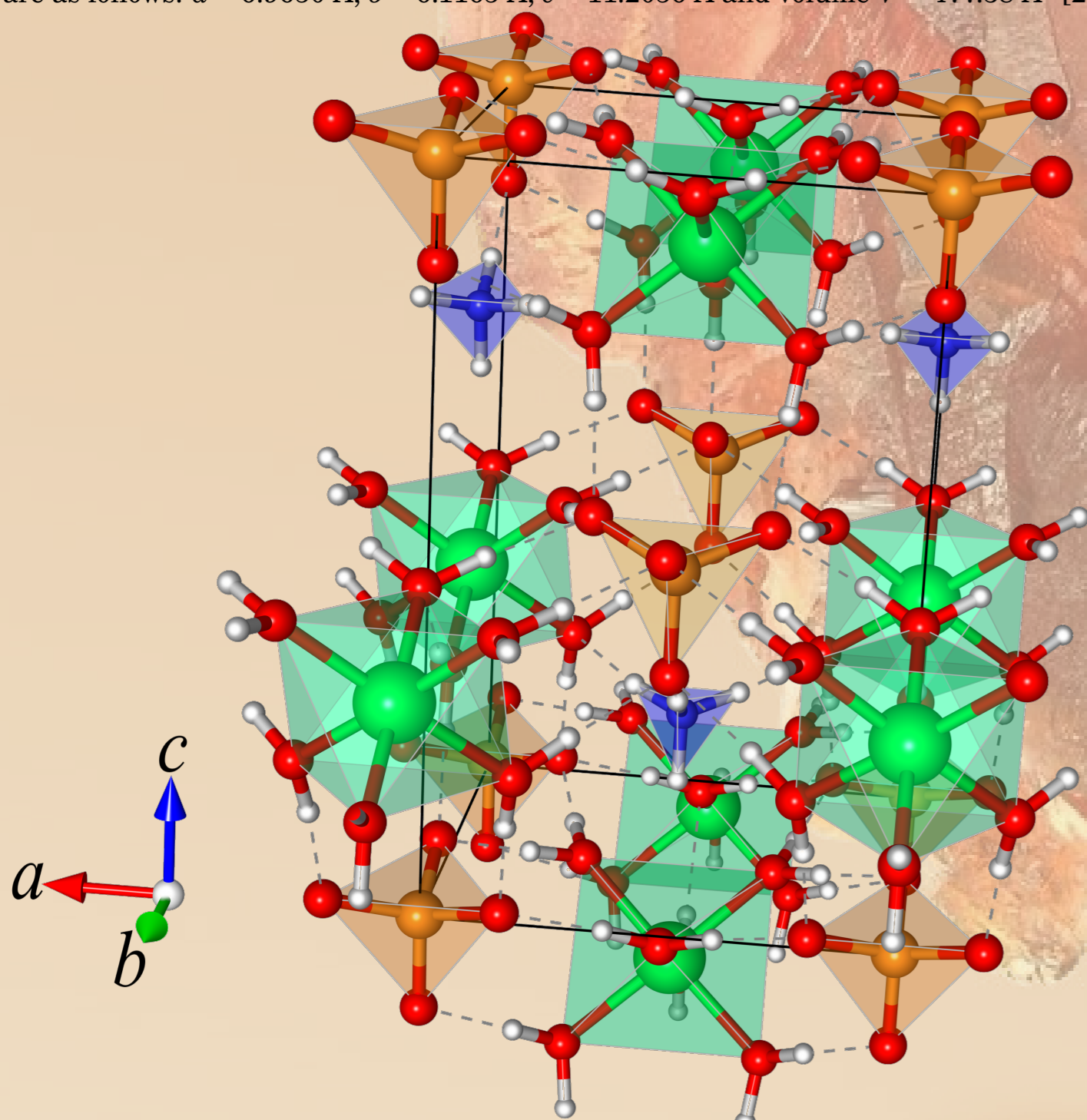


Figure 2. Primitive cell of struvite crystal, picture generated using VESTA3 software [3]. The assumed color code: white - hydrogen atoms; red - oxygen atoms; blue - nitrogen atoms in NH_4^+ tetrahedra; orange - phosphorus atoms in PO_4^{3-} tetrahedra; green - magnesium atoms in $Mg(H_2O)_6^{2+}$ octahedra.

5. Measurement of Young's modulus

Young's modulus was measured for struvite in the form of single crystal and pellet using nanoindentation technique on Nano Indenter G200 system (KLA Corporation). At least 25 experiments were performed on each sample. The crystals were examined only on the (001) surface. The indenter was applied perpendicularly to the surface (001), which means that the value of Young's modulus along the z -axis, denoted in this work by E_z , was measured. The obtained value of Young's modulus E_z for struvite crystals is 42.4 ± 3.2 GPa and for the pellet it is 23.1 ± 6.7 GPa.

6. Density Functional Theory

Calculations were carried out within the framework of the Density Functional Theory (DFT) with the CRYSTAL17 code [1]. Density functional methods, which have been shown to predict accurately lattice constants and geometry of struvite crystals, i.e. M05-2X, HISS, and B3LYP-D3^{ATM}, M06-L functionals [4], have been employed. Both functionals are adequate for description of struvite thanks to providing correct picture of covalent and molecular interaction bonding structure in this crystal. The latter is crucial in theoretical prediction of elastic properties.

Table 1. Lattice constants obtained by utilizing different functionals, compared to experimental values. MUE is a mean unsigned error for lattice constants

Functional	a [Å]	b [Å]	c [Å]	V [Å ³]	MUE [Å]
M06-L	6.940	6.085	11.153	471.02	0.036
B3LYP-D3 ^{ATM}	6.953	6.058	11.197	471.62	0.026
HISS	6.961	6.064	11.222	473.73	0.024
M05-2X	6.950	6.097	11.211	475.04	0.014
experiment*	6.965	6.171	11.206	477.37	

* obtained in our laboratory, Ref. [2].

7. Results

There are nine independent elastic constants to calculate for struvite. In Table 2 we present values of the elastic compliance matrix S_{ij} coefficients obtained using selected functionals. Notice that coefficients of the stiffness matrix C_{ij} follow from inverting the matrix S .

Table 2. Calculated elastic compliance coefficients S_{ij} in dependence of the functional used, expressed in TPa^{-1}

Functional	S_{11}	S_{22}	S_{33}	S_{44}	S_{55}	S_{66}	S_{12}	S_{13}	S_{23}
M05-2X	30.1	24.9	23.4	86.2	160.1	84.7	-13.3	-8.8	-6.8
HISS	21.1	19.2	18.3	69.1	107.6	59.0	-8.8	-5.8	-5.0
B3LYP-D3 ^{ATM}	22.6	20.0	18.8	74.2	137.4	66.5	-9.9	-6.3	-5.3
M06-L	39.2	26.6	24.0	97.4	305.9	122.5	-18.3	-10.6	-5.6

Table 3 shows a comparison for theoretically obtained Young's modulus values with the experimental value. The former were calculated on the basis of equation (1) from the coefficients of the compliances matrix S_{ij} , which are presented in Table 2. The axis x , y , and z , correspond to [100], [010], and [001] directions, respectively.

$$\frac{1}{E} = S_{11}l_1^4 + S_{22}l_2^4 + S_{33}l_3^4 + (2S_{12} + S_{66})l_1^2l_2^2 + (2S_{23} + S_{44})l_2^2l_3^2 + (2S_{13} + S_{55})l_1^2l_3^2 \quad (1)$$

Table 3. Determined values of Young's modulus expressed in GPa, compared to experimental value.

Functional	E_x [100]	E_y [010]	E_z [001]
M06-L	25.5	37.6	41.6
B3LYP-D3 ^{ATM}	44.3	50.1	53.2
HISS	47.5	52.1	54.5
M05-2X	33.2	40.1	42.7
experimental value*			42.4

* value obtained in this work, see section 5.

In Figure 3 we present Young's modulus computed for continuously varying directions.

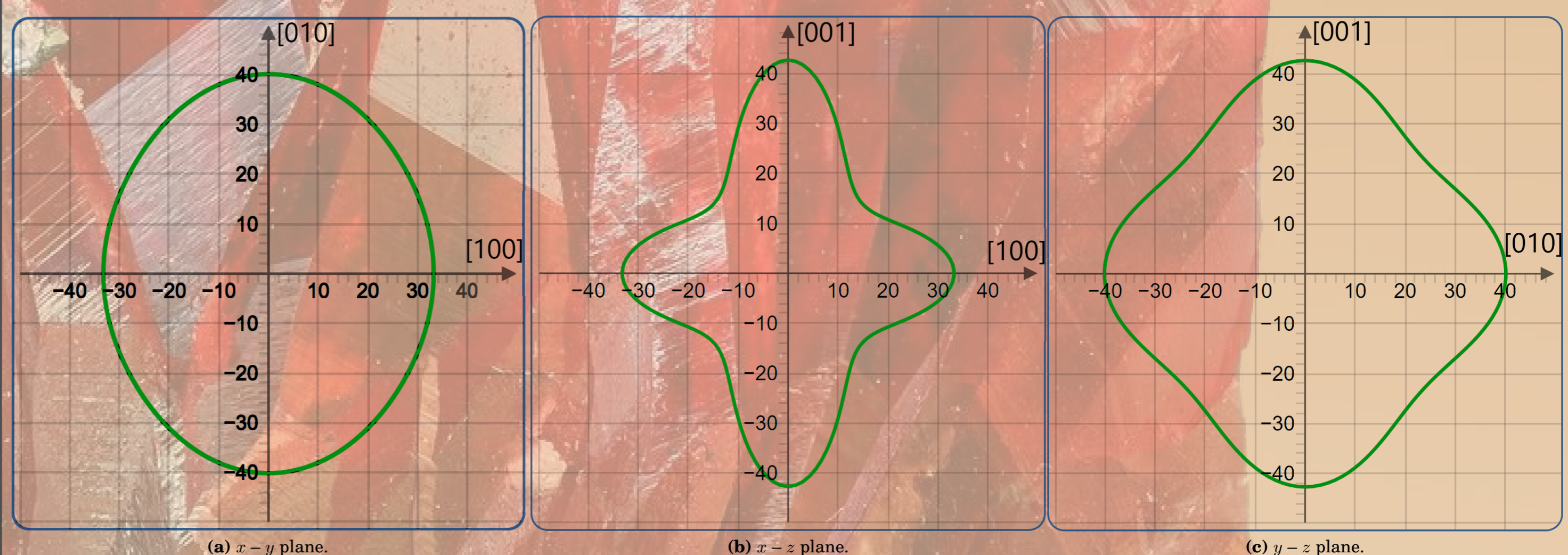


Figure 3. The value of Young's modulus in varied crystallographic directions, calculated using M05-2X functional.

For polycrystalline aggregate, the meaning of the components of the elastic and stiffness matrices is lost, and averaging over crystal orientations is necessary. In the established and recommended approach, known as Voigt-Hill-Reuss approximation (VHR), the average of Voigt and Reuss values are taken. This is justified by the proof of Hill [5], that the Voigt and Reuss assumptions represent upper and lower limits of the true polycrystalline constants. In Table 4 VHR-predicted polycrystalline elastic properties obtained with the employed density functionals are compared and confronted with the experimental values.

Table 4. Calculated polycrystalline bulk modulus B_{VHR} , shear modulus G_{VHR} , and Young's modulus E_{VHR} , expressed in GPa, compared with experimental value.

Functional	B_{VHR}	G_{VHR}	E_{VHR}
M06-L	48.9	8.4	24.0
B3LYP-D3 ^{ATM}	54.1	13.7	38.0
HISS	52.0	15.3	41.9
M05-2X	48.6	11.1	31.0
experiment [6]	49.7	11.2	31.1
experimental value*			23.1

* value obtained in this work, see section 5.

8. Conclusions

Inspection of Tables 3 and 4 reveals that the M05-2X and M06-L functionals provide elastic properties of struvite in excellent agreement with the experimental data. Notice that the agreement of the other two functionals - B3LYP-D3^{ATM} and HISS falls out of the error bars for the experimentally obtained E_z value. We confirm that M05-2X is particularly well suited to study struvite, as already reported in Ref. [4].

Good agreement of the theoretically obtained M05-2X and M06-L values with the experimental data for the z -component of the Young's modulus, E_z , for the crystal and the pellet allows us to provide estimation for E_x and E_y values as [25.5; 33.2] and [37.6; 40.1] (values in GPa), respectively. The experimental values of the E_x and E_y components of the Young's modulus have not been reported so far.

The knowledge of mechanical properties of struvite may point the manner by which urinary stones interact with the mechanical stresses produced by extracorporeal shock-wave lithotripsy - one of the most frequently used procedures for treatment of the urinary stones. All these properties can have influence on selecting of suitable parameters of ultrasonic wave to obtain the best response from the urinary stone. The knowledge of elastic properties of struvite may be also important from the perspective of breaking and removing struvite deposition in sewage treatment plants.

9. Acknowledgment

The calculations reported in this paper are performed using TUL Computing & Information Services Center infrastructure. The simulations were performed at the Interdisciplinary Centre for Mathematical and Computational Modelling, Pawińskiego 5A, PL-02-106, Warsaw.

10. References

- [1] R. Dovesi, A. Erba, R. Orlando, C.M. Zicovich-Wilson, B. Civalleri, L. Maschio, M. Rerati, S. Casassa, J. Baima, S. Salustro, B. Kirtman, Quantum-Mechanical Condensed Matter Simulations with CRYSTAL, *WIREs Computational Molecular Science*, 2018, 8, e1360.
- [2] J. Prywer, L. Sieroi, A. Czykowska, Struvite Grown in Gel, Its Crystal Structure at 90 K and Thermoanalytical Study, *Crystals*, 2019, 9, 89.
- [3] K. Momma, F. Izumi, VESTA3 for Three-Dimensional Visualization of Crystal, Volumetric and Morphology Data, *Journal of Applied Crystallography*, 2011, 44, 1272-1276.
- [4] D. Sidorczyk, M. Kozanecki, B. Civalieri, K. Pernal, and J. Prywer, Structural and Optical Properties of Struvite: Elucidating Structure of Infrared Spectrum in High Frequency Range, *Journal of Physical Chemistry A*, 2020, 124, 8668-8678.
- [5] R. Hill, The Elastic Behaviour of a Crystalline Aggregate, *Proceedings of the Physical Society, Section A*, 1952, 65, 349-355.
- [6] J. L. Katz, Elastic properties of urinary stones: some experimental and theoretical observations, *Urolithiasis: physical aspects*, Washington, DC: National Academy of Sciences, 1972, 215-235.